PROCEEDINGS OF SCIENCE

SLAC-PUB-15477

Studies of exclusive charmless semileptonic B decays and extraction of $|V_{ub}|$ at *BaBar*

Paul Taras*
Université de Montréal, Canada
on behalf of the BaBar collaboration
E-mail: taras@lps.umontreal.ca

In this talk, I shall report on recent studies at *BaBar* of the decay channels $B^0 \to \pi^-\ell^+\nu$, $B^+ \to \pi^0\ell^+\nu$, $B^+ \to \eta\ell^+\nu$, $B^+ \to \eta'\ell^+\nu$, $B^0 \to \rho^-\ell^+\nu$ and $B^+ \to \rho^0\ell^+\nu$. We obtain some of the most precise values of the total branching fractions of these decays, as well as partial branching fractions as a function of q^2 for the decay channels $B^0 \to \pi^-\ell^+\nu$, $B^+ \to \eta\ell^+\nu$ and $B^0 \to \rho^-\ell^+\nu$. In particular, the partial branching fractions for the $B^0 \to \pi^-\ell^+\nu$ channel allow us to extract values of the magnitude of the CKM matrix element $|V_{ub}|$ using three different QCD calculations. Two of these values are consistent, within large theoretical uncertainties, with the value of $|V_{ub}|$ measured in inclusive semileptonic B decays

The Xth Nicola Cabibbo International Conference on Heavy Quarks and Leptons,
October 11-15, 2010
Frascati (Rome) Italy

*Speaker.

 http://pos.sissa.it/

Work supported in part by US Department of Energy under contract DE-AC02-76SF00515.

SLAC National Accelerator Laboratory, Menlo Park, CA 94025

PoS(HQL 2010)022

1. Introduction

In the Standard model, quark flavour changes occur through weak interactions via the coupling of a W gauge boson. Such couplings are proportional to the relevant *CKM* matrix [1] elements. In particular, the probability of a b quark to decay into a u quark is proportional to $|V_{ub}|^2$. The unitarity properties of the CKM matrix can be represented by the so-called "unitarity triangle" in the $\rho-\eta$ complex plane. In this plane, the value of $|V_{ub}|$ is proportional to one of the sides of the triangle. Considering all the relevant measurements, it is clear from the wide band representing the allowed values of $|V_{ub}|$ that this matrix element is not well known. Its precise measurement would thus help constrain the description of the weak interactions as well as CP violation.

Values of $|V_{ub}|$ were recently reported [2] to be $(2.95\pm0.31)\times10^{-3}$ obtained in the study of the exclusive semileptonic B-decay, $B\to\pi\ell\nu$, and $(4.27\pm0.38)\times10^{-3}$ obtained in the inclusive semileptonic B-decay measurements. Should we take this difference of 2.7σ seriously? This question will be addressed in my talk.

2. Measurement of $|V_{ub}|$

The measurement of $|V_{ub}|$ requires the study of a $b\to u$ transition. Semileptonic $b\to u\ell\nu$ decays are best since they are much easier to understand theoretically than hadronic decays and much easier to study experimentally than purely leptonic decays because they are far more abundant. Exclusive semileptonic decays such as $B^0\to\pi^-\ell^+\nu$ and $B^+\to\eta\ell^+\nu$ involve a $b\to u$ transition.

The value of $|V_{ub}|$ is extracted from the partial branching fraction, $\Delta\mathscr{B}(q^2)$, measured as a function of q^2, the momentum transferred squared:

$$\Delta\mathscr{B}(q^2)=\frac{\tau_{B^0}|V_{ub}|^2G_F^2}{24\pi^3}\int_{q^2_{min}}^{q^2_{max}}|\vec{p}_{X_u}|^3f_+^2(q^2)dq^2, \tag{2.1}$$

in which $|\vec{p}_{X_u}|$ is a function of q^2:

$$|\vec{p}_{X_u}|=\sqrt{\frac{(m_B^2+m_{X_u}^2-q^2)^2}{4m_B^2}-m_{X_u}^2}, \tag{2.2}$$

Eq. 2.1 is often written as:

$$|V_{ub}|=\sqrt{\Delta\mathscr{B}/(\tau_{B^0}\Delta\zeta)} \tag{2.3}$$

where $\tau_{B^0}=1.530\pm0.009$ ps [3] is the B^0 lifetime and

$$\Delta\zeta=\frac{G_F^2}{24\pi^3}\int_{q^2_{min}}^{q^2_{max}}|\vec{p}_{X_u}|^3f_+(q^2)^2dq^2. \tag{2.4}$$

is the normalized theoretical partial decay rate. As can be seen in Eq. 2.4, $\Delta\zeta$ depends only on well-known quantities, except for the values of the $f_+(q^2)$ form factor and its uncertainty that are provided by a QCD calculation in a given q^2 range. It is thus clear that experimental data can discriminate between various *QCD* calculations by measuring the $\Delta\mathscr{B}(q^2)$ shape precisely.

Analysis	$\pi-\eta$ analysis	$\pi-\rho$ analysis
Luminosity on $\Upsilon(4S)$ peak	422.6 fb^{-1}	349.0 fb^{-1}
Number of $B\bar{B}$ pair events	464 millions	377 millions
q^2 evaluation	$(P_B - P_{meson})^2$	$(P_\ell + P_\nu)^2$
Cut strategy	cuts, q^2 dependent	NN, q^2 dependent
Cut selection	loose ν cuts	tighter ν cuts
Signal efficiency	8% to 15%	6% to 7%
Background/signal	11.5	6.3
$B^0 \to \pi^-\ell^+\nu$ yield	11778 ± 435	7181 ± 279
Number of q^2 bins in π mode	12	6
Systematic uncertainties	full gaussian	$\pm 1\sigma$

Table 1: Comparison of various characteristics for the two analyses reported in this talk.

Experimentally, the partial branching fractions are given by: $\Delta\mathscr{B}(q_i^2) = N_i/2\varepsilon_i N_B$, where N_i is the number of observed signal events in a given q^2 range, ε_i is the efficiency given by the Monte Carlo (MC) simulation for the same q^2 range and N_B is related to the total number of $B\bar{B}$ pairs observed, taking into account the branching fractions of the $\Upsilon(4S)$ decays.

3. Experimental method

In this talk, I shall report on two recent analyses in *BaBar* concerning exclusive charmless semileptonic B decays. In the $\pi-\eta$ analysis [4], we study three decay modes: $B^0 \to \pi^-\ell^+\nu$, $B^+ \to \eta\ell^+\nu$ and $B^+ \to \eta'\ell^+\nu$ where we measure $q^2 = (P_B - P_{meson})^2$. In the $\pi-\rho$ analysis [5], we study four decay modes: $B^0 \to \pi^-\ell^+\nu$, $B^+ \to \pi^0\ell^+\nu$, $B^0 \to \rho^-\ell^+\nu$ and $B^+ \to \rho^0\ell^+\nu$ where we measure $q^2 = (P_\ell + P_\nu)^2$. I shall concentrate on the study of the $B \to \pi\ell\nu$ mode since it leads to the most precise measurement and allows us to obtain values of $|V_{ub}|$. And I shall spend most of my time on the $\pi-\eta$ analysis since it is the most recent.

As can be seen in Table 1, we have more events in the $\pi-\eta$ analysis; the values of q^2 are determined using two methods which are in principle equivalent but which do lead to variations in the values of q^2; the use of loose ν cuts results in higher signal efficiencies and thus higher signal yields but at the expense of a larger background. This larger yield allows us to obtain the values of $\Delta\mathscr{B}$ for a larger number of q^2 bins. Finally, the systematic uncertainties are evaluated in a more conservative fashion in the $\pi-\eta$ analysis.

Both analyses use an untagged technique. This means that only one of the B mesons of the $B\bar{B}$ pair produced in the decay of the $\Upsilon(4S)$ resonance is reconstructed. Since the direction of the B meson momentum is not known precisely, we compute the values of q^2 in the Y-average frame approximation [4]. This leads to an improved q^2 resolution (0.51 GeV^2) over that obtained using the usual $\Upsilon(4S)$ frame. The two-dimensional distribution of true versus reconstructed values of q^2 yields a detector response matrix which is used to unfold the measured q^2 distribution onto the true q^2 distribution, thereby correcting these values for the reconstruction effects. Similar results are obtained in the two analyses for the q^2 resolution.

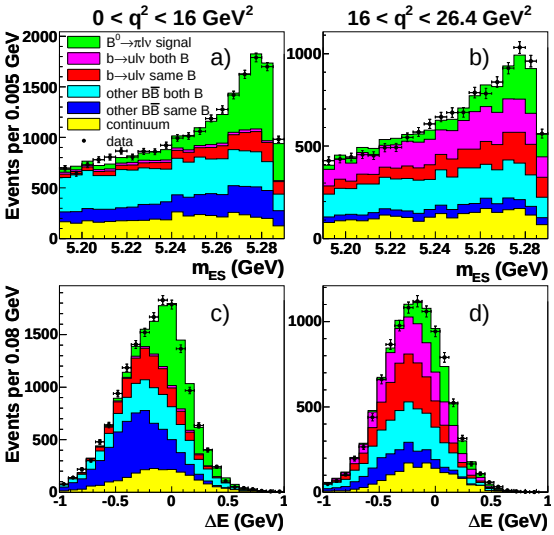

Figure 1: Projections of the data and fitted results for the $B^0 \to \pi^- \ell^+ \nu$ decays, in the signal-enhanced region: (a,b) $m_{\rm ES}$ with $-0.16 < \Delta E < 0.20$ GeV; and (c,d) ΔE with $m_{\rm ES} > 5.268$ GeV. The distributions (a,c) and (b,d) are projections for $q^2 < 16$ GeV^2 and for $q^2 > 16$ GeV^2, respectively. ($\pi - \eta$ analysis)

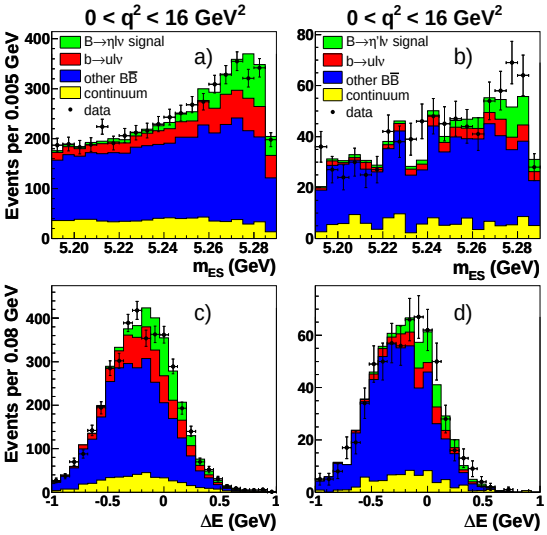

Figure 2: Projections of the data and fitted results for the $B^+ \to \eta^{(\prime)} \ell^+ \nu$ decays, in the signal-enhanced region: (a,b) $m_{\rm ES}$ with $-0.16 < \Delta E < 0.20$ GeV; and (c,d) ΔE with $m_{\rm ES} > 5.268$ GeV. The distributions (a,c) and (b,d) are projections for the $B^+ \to \eta \ell^+ \nu$ and $B^+ \to \eta' \ell^+ \nu$ decays, respectively, both for $q^2 < 16$ GeV^2. ($\pi - \eta$ analysis)

In the $\pi - \eta$ analysis, the candidate selections are optimized to maximize the ratio $S/\sqrt{(S+B)}$, where S is the number of signal events and B is the total number of background events. The use of four cuts that are q^2-dependent lead to a reconstruction efficiency which is a smoothly varying function of q^2. Backgrounds can be broadly grouped into three main categories: decays arising from $b \to u\ell\nu$ transitions (other than the signal), decays in other $B\bar{B}$ events (excluding $b \to u\ell\nu$) and decays in continuum events. For the $B^0 \to \pi^- \ell^+ \nu$ mode only, in which there are many events, each of the first two categories is further split into a background category where the pion and the lepton come from the decay of the same B, and a background category where the pion and the lepton come from the decay of different B mesons. Given the sufficient number of events in the $\pi - \eta$ analysis for the $\pi^- \ell^+ \nu$ decay mode, the data samples can be subdivided in 12 bins of q^2 for the signal and 2 bins for each of the five background categories. For the $\pi - \rho$ analysis and the $\eta^{(\prime)} \ell \nu$ modes, a smaller number of events leads us to restrict the number of bins used in the fit.

We use the ΔE-$m_{\rm ES}$ histograms, obtained from the MC simulation as two-dimensional probability density functions (PDFs), in our fit to the data, to extract the yields of the signal and backgrounds as a function of q^2. We show in Fig. 1 ΔE and $m_{\rm ES}$ fit projections in the signal-enhanced region for $B^0 \to \pi^- \ell^+ \nu$ decays in two ranges of q^2 corresponding to the sum of eight bins below and four bins above $q^2 = 16$ GeV^2, respectively. The data and the fit results are in good agreement. Fit projections for $B^+ \to \eta^{(\prime)} \ell^+ \nu$ decays, only available below $q^2 = 16$ GeV^2, are shown in Fig. 2. Table 2 shows the total fitted yields in the full q^2 range for the signal and each background category as well as the χ^2 values and degrees of freedom for the overall fit region. The fixed values are given by the MC simulation. The normalized values of χ^2 are entirely reasonable.

Decay mode	$\pi^-\ell^+\nu$	$\eta\ell^+\nu$	$\eta'\ell^+\nu$
Signal	11778 ± 435	888 ± 98	141 ± 46
$b \to u\ell\nu$	27793 ± 929	$2201(fixed)$	$204(fixed)$
Other $B\overline{B}$	80185 ± 963	17429 ± 247	2660 ± 82
Continuum	27790 ± 814	3435 ± 195	$517(fixed)$
MC events	147546 ± 467	23953 ± 183	3522 ± 68
Data events	147529 ± 384	23952 ± 155	3517 ± 59
χ^2/ndf	$411/386$	$56/52$	$19/17$

Table 2: Fitted yields in the full q^2 range for the signal and each background category, total number of MC and data events, and values of χ^2 for the fitted region in the $\pi-\eta$ analysis.

Decay mode			$\pi^-\ell^+\nu$		$\eta\ell^+\nu$	$\eta'\ell^+\nu$
q^2 range (GeV^2)	$q^2<12$	$q^2<16$	$q^2>16$	full q^2 range	$q^2<16$	$q^2<16$
Yield	6541.6	8422.1	3355.4	11777.6	887.9	141.0
BF (10^{-4})	0.83	1.09	0.33	1.42	0.36	0.24
Fit error	3.9	3.7	7.6	3.5	12.5	32.8
Detector effects	3.1	3.5	6.1	4.0	8.0	8.8
Continuum bkg	2.3	1.9	4.0	2.4	0.3	7.1
$B \to X_u\ell\nu$ bkg	2.0	1.7	4.2	2.0	7.6	6.7
$B \to X_c\ell\nu$ bkg	0.6	0.7	1.8	1.0	1.2	2.6
Other effects	2.3	2.2	3.2	2.3	3.4	4.6
Total uncertainty	6.3	6.2	12.0	6.7	17.0	35.8

Table 3: Values of signal yields, $\Delta\mathscr{B}(q^2)$ and their relative uncertainties (%) for $B^0 \to \pi^-\ell^+\nu$, $B^+ \to \eta\ell^+\nu$ and $B^+ \to \eta'\ell^+\nu$ decays in the $\pi-\eta$ analysis.

In each analysis, the systematic uncertainties are estimated from the variations of the resulting partial BF values (or total BF values for $B^+ \to \eta'\ell^+\nu$ decays) when the data are re-analyzed with different simulation parameters and reweightings. In the $\pi-\eta$ analysis, for each parameter, we use the full MC dataset to generate new ΔE-$m_{\rm ES}$ distributions ("MC event samples") by varying randomly only the parameter of interest over a complete ($> 3\sigma$) gaussian distribution whose standard deviation is given by the uncertainty on the specific parameter under investigation. One hundred such samples are generated for each parameter. Uncertainties due to B counting and final state radiation are estimated by generating only one sample. Each MC sample is analyzed the same way as real data to determine values of $\Delta\mathscr{B}(q^2)$ (or total BF values for $B^+ \to \eta'\ell^+\nu$ decays). The contribution of the parameter to the systematic uncertainty is given by the RMS value of the distribution of these values over the one hundred samples. A condensed version of all the uncertainties is given in Table 3 together with signal yields and partial BFs in selected q^2 ranges.

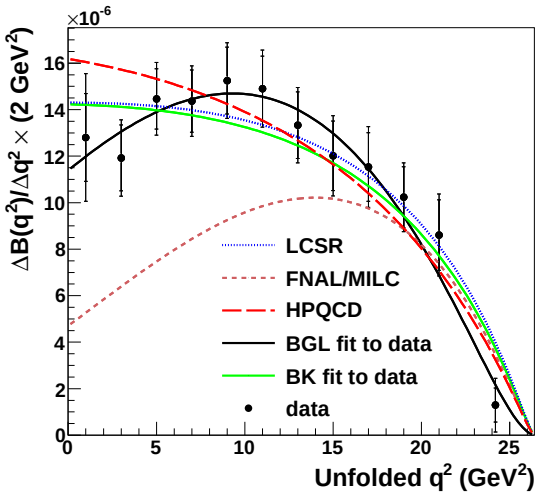

Figure 3: Partial $\Delta\mathscr{B}(q^2)$ spectrum in 12 bins of q^2 for $B^0 \to \pi^-\ell^+\nu$ decays in the $\pi-\eta$ analysis. The solid green and black curves show the result of the fit to the data of the BK [6] and BGL [7] parametrizations, respectively. The data are also compared to unquenched LQCD calculations (HPQCD [8], FNAL [9]) and an LCSR calculation [10].

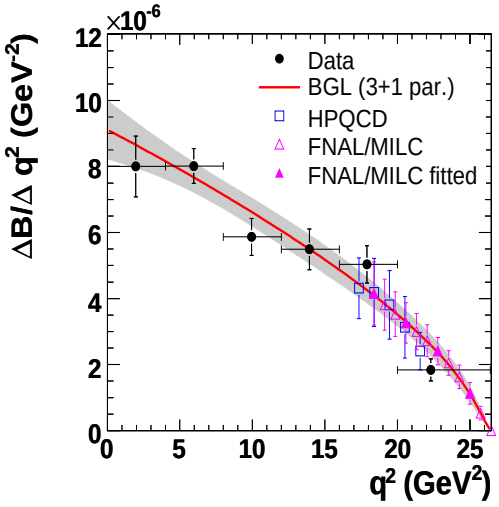

Figure 4: Partial $\Delta\mathscr{B}(q^2)$ spectrum in 6 bins of q^2 for $B^0 \to \pi^-\ell^+\nu$ decays in the $\pi-\rho$ analysis. The red curve represents the simultaneous fit to two data points and four theoretical points produced with the FNAL LQCD calculation (magenta, closed triangles).

4. Results

The experimental $\Delta\mathscr{B}(q^2)$ distributions for $B^0 \to \pi^-\ell^+\nu$ decays are displayed in Fig. 3 for the $\pi-\eta$ analysis, together with two parametrizations and three QCD calculations, and in Fig 4 for the $\pi-\rho$ analysis, combining the charged and neutral pion channels, assuming isospin symmetry. The BGL expansion gives an excellent fit to the data obtained in the $\pi-\eta$ analysis. From this fit extrapolated to $q^2=0$, we obtain the value of $|V_{ub}f_+(0)|$ in the $\pi-\eta$ analysis. This value differs from the one obtained in the $\pi-\rho$ analysis since the experimental distributions do look diffferent. However, the individual values of the partial branching fractions are indeed consistent with each other for the two analyses. The comparison between theory and experiment in their q^2 ranges of validity shows that all three calculations are compatible with the data.

We obtain the total BFs $\mathscr{B}(B^0 \to \pi^-\ell^+\nu) = (1.42 \pm 0.05_{stat} \pm 0.08_{syst}) \times 10^{-4}$, $\mathscr{B}(B^+ \to \eta\ell^+\nu) = (0.36 \pm 0.05_{stat} \pm 0.04_{syst}) \times 10^{-4}$ and $\mathscr{B}(B^+ \to \eta'\ell^+\nu) = (0.24 \pm 0.08_{stat} \pm 0.03_{syst}) \times 10^{-4}$ in the $\pi-\eta$ analysis, and $\mathscr{B}(B^0 \to \pi^-\ell^+\nu) = (1.41 \pm 0.05_{stat} \pm 0.07_{syst}) \times 10^{-4}$ and $\mathscr{B}(B^0 \to \rho^-\ell^+\nu) = (1.75 \pm 0.15_{stat} \pm 0.27_{syst}) \times 10^{-4}$ in the $\pi-\rho$ analysis. Values of $|V_{ub}|$ obtained in our two analyses are given in Table 4. They range from $(3.1-3.8) \times 10^{-3}$.

Since, in the $\pi-\rho$ analysis, the number of data points is limited to two above $q^2 = 16$ GeV^2, the range of validity of the LQCD calculations, it was deemed desirable to undertake a simultaneous fit of theoretical and experimental points to extract a value of $|V_{ub}|$. Using the FNAL calculations, we obtain in that case a lower value of $|V_{ub}|$, $(2.95 \pm 0.31) \times 10^{-3}$.

Analysis	$\pi-\eta$	$\pi-\rho$
HPQCD [8] ($q^2 > 16$ GeV^2)	$3.24 \pm 0.13 \pm 0.16^{+0.57}_{-0.37}$	$3.21 \pm 0.17^{+0.55}_{-0.36}$
FNAL [9] ($q^2 > 16$ GeV^2)	$3.14 \pm 0.12 \pm 0.16^{+0.35}_{-0.29}$	$3.07 \pm 0.16^{+0.34}_{-0.28}$
LCSR [10] ($q^2 < 12$ GeV^2)	$3.70 \pm 0.07 \pm 0.09^{+0.54}_{-0.39}$	$3.78 \pm 0.13^{+0.55}_{-0.40}$
$\lvert V_{ub} f_+(0)\rvert$	$(8.6 \pm 0.3_{stat} \pm 0.3_{syst}) \times 10^{-4}$	$(10.8 \pm 0.6) \times 10^{-4}$

Table 4: Values of $|V_{ub}| \times 10^{-3}$ derived from the form-factor calculations for the $B^0 \to \pi^- \ell^+ \nu$ decays. The three uncertainties on $|V_{ub}|$ are statistical, systematic and theoretical, respectively.

5. Summary

It is estimated that there is less than 20% overlap in the selected event samples between the two analyses reported in this talk for the $B^0 \to \pi^- \ell^+ \nu$ decay channel. It is thus very satisfying to note that there is excellent agreement between the results of the two analyses. The values of the total BFs obtained in our work are the most precise total BFs todate. Our value of the total BF for $B^+ \to \eta' \ell^+ \nu$, with a significance of 2.9σ, is an order of magnitude smaller than the CLEO result [11]. The value of the ratio $\mathscr{B}(B^+ \to \eta' \ell^+ \nu)/\mathscr{B}(B^+ \to \eta \ell^+ \nu) = 0.67 \pm 0.24_{stat} \pm 0.11_{syst}$ allows an important gluonic singlet contribution to the η' form factor. The three values of $|V_{ub}|$ are all acceptable according to the data. Two of them [8, 10] are consistent, within large theoretical uncertainties, with the value measured in inclusive semileptonic B decays: $|V_{ub}| = (4.27 \pm 0.38) \times 10^{-3}$ [3].

References

[1] M. Kobayashi and T. Maskawa, Prog. Theor. Phys. **49**, 652 (1973).

[2] B. Kowaleski, talk at FPCP 2010.

[3] K. Nakamura *et al.* (Particle Data Group), Jour. of Phys. **G37**, 075021 (2010); see also "Determination of $|V_{cb}|$ and $|V_{ub}|$", ibidem.

[4] P. del Amo Sanchez *et al.* (*BaBar* Collaboration), arXiv:1010.0987, submitted to Phys. Rev. **D**.

[5] P. del Amo Sanchez *et al.* (*BaBar* Collaboration), arXiv:1005.3288, accepted by Phys. Rev. **D**.

[6] D. Becirevic and A. B. Kaidalov, Phys. Lett. **B478**, 417 (2000).

[7] C. G. Boyd and M. J. Savage, Phys. Rev. **D56**, 303 (1997).

[8] E. Gulez *et al.* (HPQCD Collaboration), Phys. Rev. **D73**, 074502 (2006); Erratum ibid. **D75**, 119906 (2007).

[9] C. Bernard *et al.* (FNAL/MILC Collaboration), Phys. Rev. **D80**, 034026 (2009); R. Van de Water, private communication.

[10] G. Duplancic *et al.*, JHEP **804**, 14 (2008); A. Khodjamirian, private communication.

[11] S. B. Athar *et al.* (CLEO Collaboration), Phys. Rev. **D68**, 072003 (2003).